Investigation of the hydro-mechanical behaviour of compacted bentonite/sand mixture based on the BExM model

Qiong Wang, Anh Minh Tang, Yu-Jun Cui, Jean-Dominique Barnichon, Wei-Min Ye

Investigation of the hydro-mechanical behaviour of compacted bentonite/sand mixture based on the BExM model

Qiong Wang[a], Anh Minh Tang[a], Yu-Jun Cui[a,c],

Jean-Dominique Barnichon [b], Wei-Min Ye[c]

[a] *Ecole des Ponts ParisTech, Navier/CERMES, 6-8 av. Blaise Pascal, Cité Descartes, Champs-sur-Marne, 77455 MARNE LA VALLEE, France*

[b] *Institut de Radioprotection et de Sûreté Nucléaire (IRSN),* PRP-DGE/SRTG/LETIS, BP 17, Fontenay-aux-Roses, *France*

[c] *Tongji University, 1239 Siping road, 200092, China*

Corresponding author:

Prof. Yu-Jun CUI

Ecole des Ponts ParisTech

6-8 av. Blaise Pascal, Cité Descartes, Champs-sur-Marne

77455 MARNE LA VALLEE

France

Telephone: +33 1 64 15 35 50

Fax: +33 1 64 15 35 62

E-mail: yujun.cui@enpc.fr

Abstract:

This study focuses on the hydro-mechanical behaviour of a MX80 bentonite/sand mixture. Barcelona Expansive Model (BExM) was used to describe this behaviour. For this purpose, experimental data obtained in the laboratory were analysed, allowing determination of the parameters used in the model. These parameters were then used to simulate the hydro-mechanical (H-M) responses of the material from other tests with different stress paths. It was observed that the model reproduced well the main feature of swelling pressure development and micro-structural volume change during suction decrease. On the other hand, the simulations also showed some limitations of the model which is based on the consideration of two levels of soil structure or double structure: the pore size distribution curve determined by the technique of mercury intrusion porosimetry (MIP) in the range of low suctions (4.2 and 1 MPa) being revealed to be tri-modal, the BExM model cannot capture this aspect to correctly describe the macro-structural and micro-structural void ratio changes. Moreover, because the BExM model lumps clay intra-particle spaces and inter-particles voids together as micro-pores, it leads to overestimation of the micro-structural water content compared to the experimental value.

Keywords: bentonite/sand mixture; hydro-mechanical behaviour; constitutive modeling; volume change; microstructure.

1 INTRODUCTION

Compacted bentonite-based materials have been proposed as engineering barriers in the deep geological repository for high-level radioactive wastes (HLW) in several countries. Thanks to their low permeability, high swelling and high radionuclide retardation capacities [1-3], they are expected to limit the release of radionuclide to the surrounding host rock [4]. After installation in the repository, the engineering barriers will simultaneously undergo the intrusion of groundwater from the host rocks or geological barriers, and the stress changes mainly due to the bentonite swelling. Therefore, the hydro-mechanical performance of engineering barriers is a key issue in assessment of the overall repository safety.

Various laboratory studies have been conducted on the H-M behaviour of bentonite-based materials [5-9]. Based on the experimental results, a number of constitutive models have been developed such as the model of Gens and Alonso [10], the model of Alonso et al. [11] and the model of Cui et al. [12], etc. To the authors' knowledge, the elasto-plactic model developed by Alonso et al. [11], namely Barcelona Expansive Model (BExM), is the most widely used one in describing the mechanical behaviour of unsaturated expansive soils.

In the BExM model, the authors incorporate the microstructure effects by introducing two levels of soil structure: a microstructure level that corresponds to the active clay minerals with prevailing physico-chemical effects, and a macrostructure level that accounts for the larger scale structure of the soil. The coupling between the two levels is

described by means of the interaction functions capable of describing, in a phenomenological fashion, the occurrence of macro-structural elasto–plastic strains as a consequence of micro-structural strains.

Because of the complexity of the model, there have been few experimental works that allow the determination of the full set of its parameters, especially for the bentonite-based materials. In this study, the hydro-mechanical behaviour of compacted MX80 bentonite/sand mixture was investigated based on the BExM model. The determination of the model parameters was first conducted by matching the model equations with the laboratory experimental results. The parameters thus determined were then used to simulate the H-M behaviour of the material in the swelling pressure and water retention tests. The performance and limitation of the model were further analysed by comparing the model and experimental results and by considering the microstructure changes upon wetting or suction decrease.

2 BARCELONA EXPANSIVE MODEL

As mentioned previously, Barcelona Expansive Model (BExM) proposed by Alonso et al. [11] accounts for two levels of soil structure [10, 13]: micro- and macro-structural levels. The micro-structural level corresponds to the aggregates of active clay particles with intra-aggregate pores, whereas the macro-structural level corresponds to the larger scale soil structure [14-15]. Following this concept, the void ratio (e) can be split into two parts:

$$e = e_m + e_M \tag{1}$$

where e_m and e_M are micro- and macro-structural void ratios, respectively.

The micro-structural pores are assumed to be always saturated, thus the Terzaghi's effective stress concept holds: any given changes in suction (s) induce the same volume change as that induced by the same changes in mean net stress (p). The volume change in this level is reversible and independent of macro-structural effects [10]. Thereby, the micro-structural elastic volumetric strain is calculated as follows:

$$d\varepsilon_{vm}^{e} = \frac{de_m}{1+e_m} = \frac{d(p+s)}{K_m} \tag{2}$$

$$\text{with} \quad K_m = \frac{\exp[\alpha_m (p+s)]}{\beta_m} \tag{3}$$

where K_m is the micro-structural modulus; it increases with increase in p or s. α_m and β_m are model parameters which define the micro-structural bulk modulus K_m.

In the macro-structural level, both elastic and plastic strains can develop as a result of stress/suction changes. The macro-structural elastic volumetric strain is expressed as a function of mean net stress and suction:

$$d\varepsilon_{vM}^{e} = \frac{de_M}{1+e_M} = \left(\frac{\kappa}{1+e_M}\right)\frac{dp}{p} + \left(\frac{\kappa_s}{1+e_M}\right)\frac{ds}{s+p_{atm}} \tag{4}$$

where κ and κ_s are the macro-structural elastic compressibility parameters for changes in stress and in suction, respectively, p_{atm} is the atmospheric pressure.

The variation of pre-consolidation mean net stress (p_0) with suction is given by an LC (Loading Collapse) yield curve function in the (p, s) plane (Figure 1):

$$\frac{p_0}{p_c} = \left(\frac{p_0^*}{p_c}\right)^{\frac{\lambda(0)-\kappa}{\lambda(s)-\kappa}} \tag{5}$$

112 $$\text{with} \quad \lambda(s) = \lambda(0)\left[r + (1-r)\exp(-\beta s)\right] \tag{6}$$

113 where p_c is a reference stress, p_0^* is the net mean yield stress at zero suction, $\lambda(0)$ is the
114 macro-structural compressibility parameter for changes in p at zero suction (saturated
115 state), $\lambda(s)$ is the macro-structural compressibility parameter for changes in p at suction
116 s, r is a parameter that defines the minimum compressibility of soil and β is a parameter
117 that controls the rate of compressibility decrease with increasing suction.

118 The micro-structural deformations-induced plastic strains are described by two
119 additional yield curves SI (suction increase) and SD (suction decrease) in Figure 1. The
120 SI yield curve is defined by the expression $p + s_I = 0$ and the SD yield curve is defined
121 by the expression $p + s_D = 0$ where s_I, s_D are both hardening parameters. For a reason of
122 simplicity, it is assumed that the SI and SD yield curves are always activated thereby
123 inducing irreversible macro-structural deformations. Under this assumption the SI and
124 SD curves are masked by the Neutral Line (NL). Note that Alonso et al. [15], Sánchez
125 et al. [16], Tang and Cui, [17] also considered the NL solely to separate micro-structural
126 swelling from micro-structural compression. Upon hydro-mechanical loadings, the NL
127 moves following the current stress (p) and current suction (s). Therefore, the following
128 two parts of irreversible volumetric strains are taken into account:
129 1) When the yield curve LC is reached by a mechanical loading:

130 $$d\varepsilon_{vML}^{p} = \frac{\lambda(s) - \kappa}{1 + e_M} \frac{dp_0}{p_0} \tag{7}$$

131 2) As mention above, the SI and SD yield curves are assumed to be always activated,
132 the macro-structural plastic strain induced by micro-structural strain is:

$$d\varepsilon^{p}_{vMSI} = f_I d\varepsilon^{e}_{vm} \tag{8}$$

$$d\varepsilon^{p}_{vMSD} = f_D d\varepsilon^{e}_{vm} \tag{9}$$

where f_I and f_D are the interaction functions between micro- and macro-structural levels in case of suction increase and suction decrease, respectively.

Regarding the hardening law for LC yield curve, the yield stress at zero suction (p_0^*) is expressed as a function of the total macro-structural strain (ε^p_{vM}).

$$\frac{dp_0^*}{p_0^*} = \frac{(1+e_M)d\varepsilon^p_{vM}}{\lambda(0)-k} \tag{10}$$

Note that the increment of the total macro-structural plastic strain ($d\varepsilon^p_{vM}$) is the sum of the increment of the macro-structural plastic strain resulted by hydraulic and mechanic loading ($d\varepsilon^p_{vML}$) and that resulted by the micro-structural interactions ($d\varepsilon^p_{vMSI}$ or $d\varepsilon^p_{vMSD}$), as follows:

$$d\varepsilon^{p}_{vM} = d\varepsilon^{p}_{vML} + d\varepsilon^{p}_{vMSI} + d\varepsilon^{p}_{vMSD} \tag{11}$$

3 PARAMETERS DETERMINATION

The model parameters were determined on the basis of the experimental results obtained on the MX80 bentonite/sand mixture. The soil microstructure was investigated using mercury intrusion porosimetry (MIP) by Wang et al. [18], and the results allow determining the initial micro- and macro-structural void ratios (e_m and e_M). Montes-H et al. [20] investigated the swelling of a single clay aggregate under relative humidity changes using the technique of environmental scanning electron microscopy (ESEM) in conjunction with a digital image analysis. The observed volume changes

were used to calibrate the variation of e_m with suction changes. The volume changes upon wetting and loading were studied by carrying out suction controlled oedometer tests [18]. The results obtained were used for the determination of the model parameters related to the hydro-mechanical behaviour. It is important to note that the notation "*p*" used in the BExM refers to "mean stress". As the results from oedometers tests were considered for parameters' determination. In the following, the notation "*p*" used refers to the vertical stress in oedometer condition.

Figure 2 depicts the pore size distribution (PSD) curve of the compacted MX80 bentonite/sand mxiture having an initial suction of 65 MPa and a void ratio of 0.635. The incremental pore volume was represented by the change of void ratio *e* divided by the change of the logarithm of pore diameter *d*: d*e*/dlog*d*, corresponding to the total volume of the pores having similar entrance pore diameter *d*. A clear double structure can be observed, defining a population of intra-aggregate pores (micro-pores) with a mean size of 0.02 μm and a population of inter-aggregate pores (macro-pores) with a mean size of 50 μm. The inter-aggregates pores were found to be dependent on dry density, while the intra-aggregate pores remain unaffected by the compaction [8]. Based on this evidence, a delimiting value of 2 μm between macro-pores and micro-pores for the MX80 bentonite/sand mixture was defined by Wang et al. [18] from the PSD curves of different dry densities. Thus, the micro-structural and macro-structural void ratios can be determined using the limit pore diameter of 2 μm: $e_m = 0.391$ and $e_M = 0.244$, as noted in Figure 3.

Regarding the micro-structural volume change, Montes-H et al. [20] examined the

swelling potential of a single MX80 aggregate at different relative humidity states using environmental scanning electron microscopy (ESEM) and the technique of digital image analysis. From an initial relative humidity of 2.5%, corresponding to 537 MPa suction, various relative humidity values were applied. The deformations are shown in Figure 3 versus suction (deduced from the corresponding relative humidity and temperature applied). Note that the result at the relative humidity of 95% was not taken into account due to the "water over-saturation of aggregate" appeared in the experiment [20]. The data show that wetting from the initial suction of 537 MPa to a suction of 13.5 MPa (90% relative humidity) induced a micro-structural volumetric swelling of 21%.

Based on the evidence that the swelling of mixture is totally controlled by bentonite and sand being inert [18,21,22], the experimental data obtained from MX80 bentonite by Montes-H et al. [20] were used to calibrate parameters α_m and β_m which define the micro-structural bulk modulus K_m (Eq. (2) and (3)). The changes of mixture void ratio were determined from the corresponding void ratio of pure bentonite based on the expressions shown in [18], (Eq (5) and (6)). The following parameters were used to fit the micro-structural volumetric strain to the experimental data: α_m = 0.083 MPa^{-1} and β_m = 0.011 MPa^{-1}. Starting from the initial suction of s_0 = 65 MPa (black dot in Figure 3) with the initial micro-structural void ratio of e_m = 0.391, both the wetting and drying paths were considered: e_m reduced to 0.301 at suction = 537 MPa and increased to 0.474 at suction = 0.1 MPa. With the parameters thus determined, the model can satisfactorily fit the experimental results (Figure 3).

The volume changes of compacted MX80 bentonite/sand mixture upon wetting and

197 loading were investigated by carrying out suction controlled oedometer tests (Wang et
198 al. [18]). The stress paths followed are presented in Figure 4. Three tests were
199 conducted on samples with an initial dry density of 1.67 Mg/m^3 (e = 0.635) under
200 controlled suctions. From the initial state (p_{ini} = 0.1 MPa, s = 65 MPa), suctions of 38
201 MPa, 12.6 MPa, 4.2 MPa were first applied by the vapour equilibrium technique under
202 a low vertical stress of 0.1 MPa, allowing the development of vertical swelling strain.
203 After completion of the swelling strain at each suction, loading (up to 30 MPa) was
204 applied under constant suction condition. An additional test at zero suction was
205 conducted by considering an annular void between sample and ring. The sample with a
206 diameter smaller than that of the oedometer cell was used for this purpose (see [18] for
207 more details).

208 The final void ratio values after suction equilibrium following wetting path are
209 presented in Figure 5. Due to the annular void that allowed the sample swell in the
210 radial direction, the sample undergoes first a stress path close to the isotropic conditions.
211 The significant interaction between micro- and macro-structural levels in this condition
212 leads to larger volumetric strain as compared to the oedometer condition for other tests.
213 Therefore, these results for 38 MPa, 12.6 MPa, 4.2 MPa suction were used to calibrate
214 the parameters related to the macro-structure changes due to suction decrease. Upon
215 wetting, the macro-structural behaviour involves two mechanisms: (i) elastic
216 volumetric strain (Eq. (4)) which depends on parameter κ_s; (ii) plastic volumetric strain
217 induced by the micro- and macro-structural interaction (Eq. 9) which depends on f_D. For
218 simplicity, the elastic volumetric strain (Eq. (4)) was assumed to be insignificant for the

high expansive soil considered, and a small value of κ_s = 0.001 was given. Note that the suction-induced macro-structural elastic deformation was ignored (i.e. κ_s = 0) in the work of Alonso et al. (2005). The micro-structural void ratio was calculated using the parameters determined above (α_m and β_m). The f_D was then determined by matching the void ratio values in Figure 5 with Eq. 4 and Eq.9: f_D = 0.8-1.1tanh [20×(p/p_0-0.25)].

The parameters that control the hydro-mechanical behaviour can be obtained based on the compression curves at different constant suctions. The compression curves at 4.2 MPa, 12.6 MPa and 38 MPa suction are depicted in Figure 6. From these curves the values of λ(4.2), λ(12.6), λ(38), p_0 (4.2), p_0 (12.6), p_0 (38) and κ can be determined. By using data of λ(s), parameters λ(0), γ, β can be obtained through Eq. (6) and the following values were obtained: λ(0) = 0.14, r = 0.82, β = 0.07. With these parameters determined, p_0^*, p_c were then determined by fitting the data in terms of p_0 (s): p_0^* = 0.92, p_c = 0.005. Afterwards, the f_I (in Eq.8) was obtained by matching the experimental compression curves: f_I = 0.05-1.1tanh [20×(p/p_0-0.25)]. Note that during the mechanical loading, the following volumetric strains were taken into account: ε^e_{vm} (Eq. 2), ε^e_{vM} (Eq. 4), ε^p_{vML} (Eq. 7) and ε^p_{vMSI} (Eq.8).

A summary of the model parameters thus determined and the initial conditions is given in Table 1.

4 SIMULATION AND INTERPRETATION

4.1 Swelling pressure development during suction decrease

The evolution of swelling pressure during suction decrease was simulated by applying

240 the back compaction method [23]. Following this method, the computation of swelling
241 induced stress can be performed in two stages at a certain suction and stress state
242 (Figure 7): 1) to calculate the micro-porosity change and the macro-volume change
243 potential by allowing swell in the first stage; 2) to press the swelling strain back and
244 calculate the resulting stress after the compression process. From the initial state (p_{ini} =
245 0.1 MPa, e = 0.635, s = 65 MPa), the simulation decreased the suction of the sample to
246 0.1 MPa in a series of steps at constant volume conditions. In each step, the back
247 compaction process was considered as an inverse process of swelling. Thus, the
248 predicted increase in swelling pressure can be obtained. The deformation under both
249 swelling process and compression process was assumed to be elasto-plastic. The SI and
250 SD yield curves were always activated; the loading induced plastic deformation of
251 macro-pores occurs during wetting when the yield curve LC was reached.

252 The predicted swelling pressure induced by suction decrease within the soil sample is
253 presented in Figure 8, along with the swelling pressure measured at different suctions
254 (Figure 8). The swelling pressure evolution observed in the laboratory can be well
255 reproduced by considering the occurrence of two concurrent phenomena: initially,
256 when suction is reduced the bentonite aggregates swell and a net pressure increment is
257 developed to maintain a constant volume condition. During this initial stage, the stress
258 path is far from the LC yield curve (Figure 8). However, the progressive wetting may
259 bring the stress state to the LC yield curve and the overall macrostructure is prone to
260 undergo collapse. Both phenomena co-exist during the wetting path. As noted by
261 Gens & Alonso [10] and Alonso et al. [15], if collapse strains tend to dominate over

other contributions to the total volumetric deformation, the stress path will closely follow the LC yield locus. A continuous increasing swelling pressure observed in this study indicates that the macro-pores collapse was fully compensated by the micro-structural swelling; thus no decrease in macro-pores was observed.

4.2 Microstructure changes during suction decrease

During the swelling pressure simulation under constant volume conditions, the changes of macro- and micro-structural void ratios were calculated at the end of each stage, as shown in Figure 9. The measured values from the MIP results were also presented. The correspondence between the measured and predicted deformations is reasonably good for both micro- and macro-pores, except in the case of suction of 4.2 and 1 MPa where the macro-pores quantity increased again with further suction decrease. The discrepancy was caused by the complexity of microstructure at these suctions (Figure 10): when saturation is approached ($s < 4.2$ MPa), the macro-pores observed at higher suction are filled by the swollen bentonite, however, a large quantity of fissure-like (with very large aspect ratio) 2-dimension pores (2-D pores in Audiguier et al. [24]) with mean entrance diameter of 50 μm appeared due to the division of aggregates (Figure 11a), leading to the increase of macro-pores. Moreover, a new pore group of 2-D pores of about 1 μm diameter was formed due to the fissuring of aggregates (Figure 11b), leading to a tri-modal pore size distribution [19]. Note that the MIP results obtained from wetted samples by Romero et al. (2011) also showed the complexity of the microstructure changes during wetting, with a new pore population appearing between micro- and macro-pores [25]. Obviously, the two-level soil structure,

micro-structural (intra-aggregate) and macro-structural (inter-aggregate), defined in the BExM model cannot describe this phenomenon.

4.3 Water retention property

As mentioned previously, the BExM model assumes that the micro-pores remain always saturated, thus the Terzaghi's effective stress concept holds. Following this assumption, the amount of water in the micro-pores can be calculated based on the micro-structural void ratio. The changes in micro-structural water content (w_{em}) upon wetting were calculated and are presented in Figure 12, together with the experimental water retention curve (WRC, including both micro-structural and macro-structural waters) determined using vapour equilibrium and osmotic techniques at constant volume conditions [18,19]. The model depicts well the two regions with different water retention mechanisms: intra-aggregate and inter-aggregate region. The simulated micro-structural water content curve and the measured WRC intersect at about 4-5 MPa, indicating that from this point on, the suction–water content relationship was controlled by the inter-aggregate pores. Note that this threshold suction is also close to that observed by Yahia-Aissa et al. [26] on FoCa 7 clay (3-4 MPa) and Cui et al. [27] on the mixture (7/3 by dry mass) of Kunigel V1 bentonite/Hostun sand (4-5 MPa).

On the other hand, the estimated micro-structural water content (w_{em}) was found to be higher than the water content corresponding to the WRC in the intra-aggregate region. This discrepancy is due to the micro-pores that were unsaturated in reality but assumed to be saturated in the BExM model. By considering the two levels of soil structure [10], the BExM model lumps the intra-particles (inter-layer) space and the inter-particles

306 space together as intra-aggregates pores. Actually, the intra-particles pores can be
307 considered as saturated in the range of suctions of practical interest because it requires
308 an extremely high level of suction (of the order of 10^5 kPa) to remove water from the
309 inter-layer space. However, air can enter the intra-aggregate pores (< 2 μm for the
310 bentonite/sand mixture as shown in Figure 3) at a suction of about 140 kPa, and hence
311 the corresponding voids can become unsaturated [28], leading to the discrepancy
312 between the experimental and estimated value of micro-structural void ratio. It should
313 be noted that in spite of this assumption, the model can predict well the main features of
314 volumetric strain, swelling pressure evolution etc. of expansive soils. For the
315 desaturation of micro-pores, the authors think that the model could be improved by
316 considering degree of saturation as proposed by Romero et al (2011)[25].

317 # 5 CONCLUSION

318 The hydro-mechanical behaviour of a compacted MX80 bentonite/sand mixture was
319 investigated within the framework of the Barcelona Expansive Model (BExM). The
320 model parameters were first determined based on the experimental results obtained.
321 The changes of swelling pressure, micro-structural volume change and micro-structural
322 water content were then simulated and compared with the experimental results.

323 The swelling pressure observed under constant volume was well reproduced by the
324 model. A continuous increasing swelling pressure observed indicates that the
325 macro-pores collapse was fully compensated by the micro-structural swelling.

326 The macro- and micro-structural void ratio changes upon wetting under constant

volume condition were well reproduced in the range of high suctions. However, the model cannot well describe the changes in the range of low suctions (4.2 and 1 MPa). Further examination showed that the pore size distribution curve in the low suction range is tri-modal, different from the assumption of bi-modal distribution in the BExM model.

The model depicts well the two regions of different water retention mechanisms: intra-aggregate and inter-aggregate regions. However, the predicted micro-structural water content was found higher than the water content corresponding to the WRC in the intra-aggregate region. This discrepancy is due to the micro-pores assumed to be always saturated in the BExM model, but unsaturated in reality.

On the whole, the main features of the hydro-mechanical behaviour of bentonite/sand mixture can be described by the BExM model, demonstrating the performance of this model in representing the H-M behaviour of bentonite-based materials. However, further considerations should be done when applying the model such as the formation of a third pore population under suction decrease and the de-saturation of intra-aggregate pores at high suctions.

ACKNOWLEDGEMENTS

The work was conducted in the framework of the SEALEX project of IRSN and the PHC Cai Yuanpei project (24077QE). The support of the China Scholarship Council (CSC) is also greatly acknowledged.

REFERENCES

[1] Pusch, R. Highly compacted sodium bentonite for isolating rock-deposited radioactive waste products. Nucl. Technol. (United States), 45(2) (1979):153-157

[2] Yong, R.N., Boonsinsuk, P., and Wong, G. Formulation of backfill material for a nuclear fuel waste disposal vault. Canadian Geotechnical Journal, 23(2) (1986):216-228.

[3] Villar, M.V., Lloret, A. Influence of dry density and water content on the swelling of a compacted bentonite. Applied Clay Science, 39(1-2) (2008):38-49.

[4] Cho, W.J., Lee, J.O., Kwon, S. Analysis of thermo-hydro-mechanical process in the engineered barrier system of a high-level waste repository. Nuclear Engineering and Design. 240(2010):1688-1698.

[5] Delage, P., Howat, M. D., & Cui, Y. J. The relationship between suction and swelling properties in a heavily compacted unsaturated clay. Engng Geol. 50(1) (1998): 31 – 48.

[6] Lloret, A., Villar, M. V., Sanchez, M., Gens, A., Pintado, X. & Alonso, E. E. Mechanical behaviour of heavily compacted bentonite under high suction changes. Géotechnique 53(1) (2003): 27-40

[7] Romero, E., Villar, M. V. & Lloret, A. Thermo-hydro-mechanical behaviour of heavily overconsolidated clays. Engng Geol. 81(3) (2005): 255 – 268.

[8] Lloret, A. & Villar, M. V. Advances on the knowledge of the thermo-hydromechanical behaviour of heavily compacted « FEBEX » bentonite. Physics and Chemistry of the Earth 32(8 – 14) (2007): 701 – 715.

[9] Agus, S.S., Arifin, Y. F., Tripathy, S., Schanz, T. Swelling pressure–suction relationship of heavily compacted bentonite–sand mixtures. Acta Geotechnica, DOI:10.1007/s11440-012-0189-0.

[10] Gens, A. & Alonso, E. E. A framework for the behaviour of unsaturated expansive clays. Can. Geotech. J. 29(6) (1992): 1013 – 1032.

[11] Alonso, E. E., Vaunat, J. & Gens, A. Modelling the mechanical behaviour of expansive clays. Engng Geol. 54(1) (1999): 173 – 183.

[12] Cui Y.J., Yahia-Aissa M. and Delage P. A model for the volume change behaviour of heavily compacted swelling clays. Engineering Geology 64 (2-3) (2002), 233-250.

[13] Alonso, E. E., Gens, A., Josa, A. (1990). A constitutive model for partially saturated soils. Geotechnique, 40 (3): 405–430.

[14] Kröhn, K. P. New conceptual models for the resaturation of bentonite. Applied Clay Science, 23(1 – 4) (2003): 25 – 33.

[15] Alonso, E. E., Alcoverro, J., Coste, F., et al. The FEBEX benchmark test: case definition and comparison of modelling approaches. International Journal of Rock Mechanics & Mining Science 42(5-6) (2005): 611 – 638.

[16] Sánchez, M., Villar, M. V., Gens, A., Olivella, S. & do N. Guimaraes, L. Modelling the effect of temperature on unsaturated swelling clays. Proc. of the 10th International Symposium on Numerical Models in Geomechanics (Numog X), Rhodes, Greece, (2007): 57-62.

[17] Tang, A. M., Cui, Y. J. Modelling the thermomechanical volume change behaviour of compacted expansive clays. Géotechnique, 59 (2009): 185-195

[18] Wang, Q., Tang, A. M., Cui, Y.J., Delage, P., Barnichon, J.D., & Ye, W.M. The effects of technological voids on the hydro-mechanical behaviour of compacted bentonite-sand mixture. Soils and Foundations, Vol.53, No.2 (2013) in Press.

[19] Wang, Q., Tang, A. M., Cui, Y.J., Delage, P., Barnichon, J.D., & Ye, W.M. Hydraulic conductivity and microstructure changes of compacted bentonite/sand mixture during hydration. (2012) submitted to Engineering Geology.

[20] Montes-Hernandez, G., Duplay, J., Martinez, L. & Mendoza, C. Swelling-shrinkage kinetics of MX80 bentonite. Applied Clay Science, 22(6) (2003): 279 – 293.

[21] Karnland, O., Nilsson, U., Weber, H., and Wersin, P. Sealing ability of Wyoming bentonite pellets foreseen as buffer material-Laboratory results. Physics and Chemistry of the Earth, Parts A/B/C, 33(2008), S472-S475.

[22] Wang Q., Tang A.M., Cui Y.J., Delage P., Gatmiri B. Experimental study on the swelling behaviour of bentonite/claystone mixture. Engineering Geology 124 (2012), 59-66.

[23] Xie, M. L., Wang, W. Q., De-jonge, J., and Kolditz O. Numerical Modelling of Swelling Pressure in Unsaturated Expansive Elasto-Plastic Porous Media. Transport in Porous Media, 66 (2007):311–339

[24] Audiguier, M., Geremew, Z., Cojean, R. Relations enter les microstructures de deux sols argileux de la région parisienne et leur sensibilité au retrait gonflement. SEC2008, Sécheresse et constructions, Paris, France, 1-3 sept. Editions du LCPC(2008), 235-243.

[25] Romero, E., G. Della Vecchia, C. Jommi,. An insight into the water retention properties of compacted clayey soils. Géotechnique. 61 (4) (2011): 313-328.

[26] Yahia-Aissa, M.,Delage, P., Cui, Y.J. In: Adachi, Fukue (Ed.), Suction–water Relationship in Swelling Clays, Clay Science for Engineering, IS-Shizuoka Int Symp on Suction, Swelling, Permeability and Structure of Clays. In Balkema, (2001): 65–68.

[27] Cui, Y. J., Tang, A. M., Loiseau, C., Delage, P. Determining water permeability of compacted bentonite–sand mixture under confined and free-swell conditions. Physics and Chemistry of the Earth, 33(2008): S462–S471.

[28] Sharma, R.S. Mechanical behaviour of unsaturated highly expansive clays. University of Oxford. PHD thesis (1998).

List of Tables

List of Figures

Table 1. Parameters used in the simulation

Initial state		Hydro-mechanical behaviour	
e	0.635	κ	0.006
e_m	0.391	κ_s	0.001
e_M	0.244	$\lambda(0)$	0.14
s_0	65 MPa	p_c	0.005
p_{ini}	0.1 MPa	r	0.82
p_0^*	0.92 MPa	β	0.07
		α_m	0.083 MPa^{-1}
		β_m	0.011 MPa^{-1}
		$f_D = 0.8\text{-}1.1\tanh[20\times(p/p_0\text{-}0.25)]$.	
		$f_I = 0.05\text{-}0.8\tanh[20\times(p/p_0\text{-}0.25)]$	

445

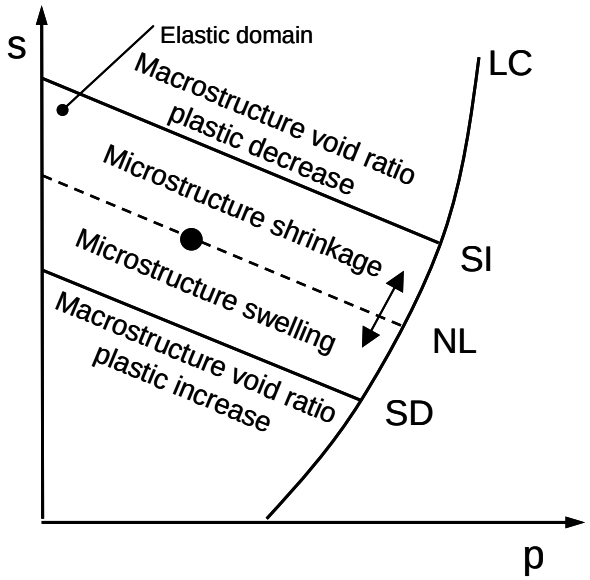

446

447 Figure 1. BExM yield loci in the *p*-*s* plane (after Alonso et al. 2005)

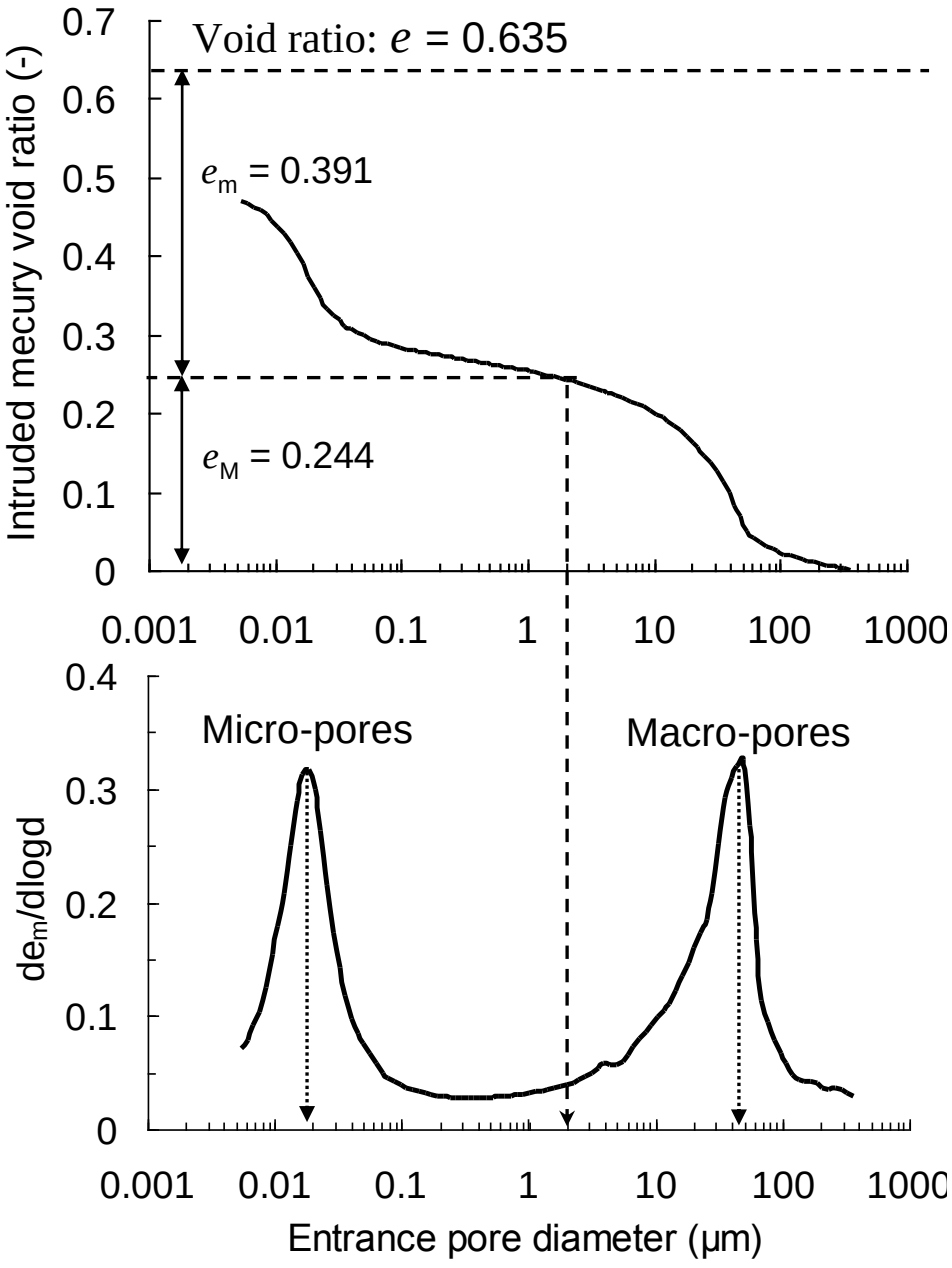

448

449 Figure 2. Pore size distribution of the compacted MX80/sand mixture

450

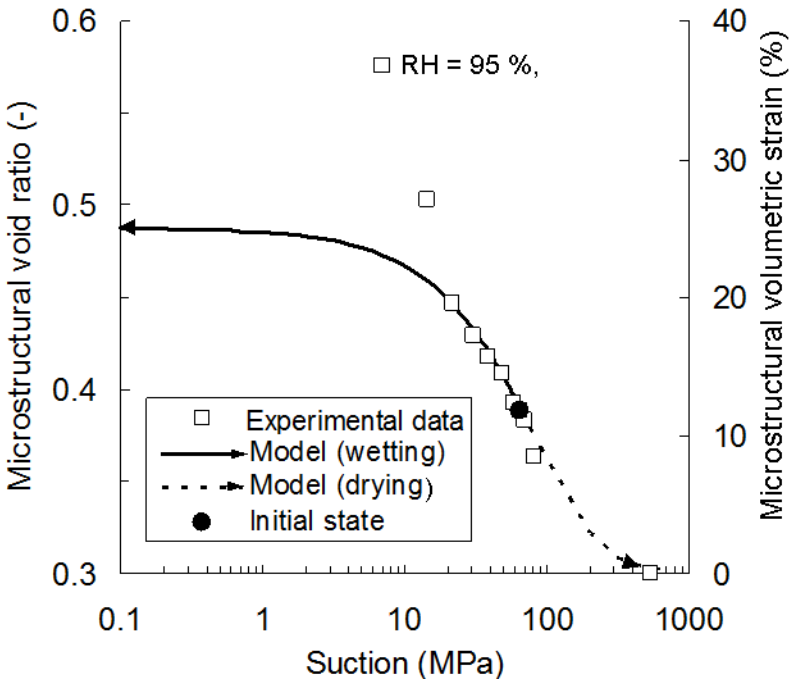

451

452 Figure 3. Micro-structural volumetric strain of MX80 bentonite and micro-structural void ratio
453 of mixture versus suction

454

455

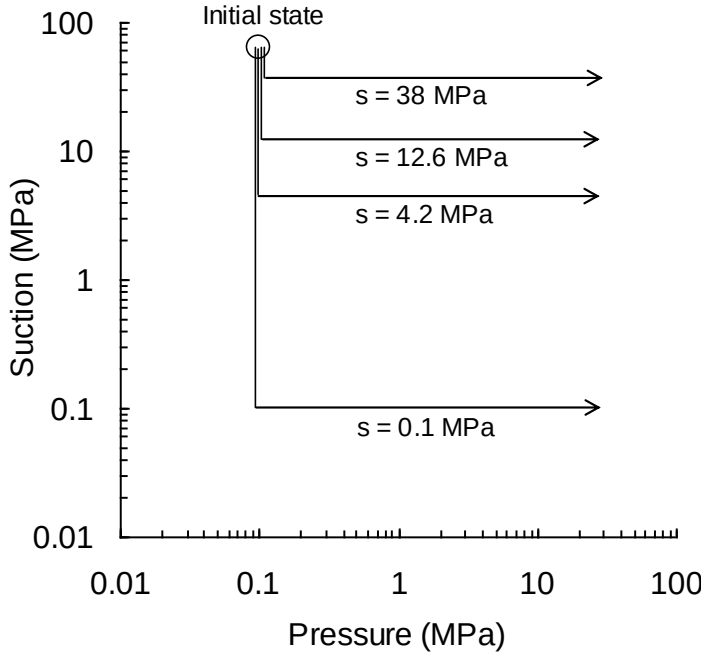

456

457 Figure 4. Stress paths followed in the suction controlled oedometer tests

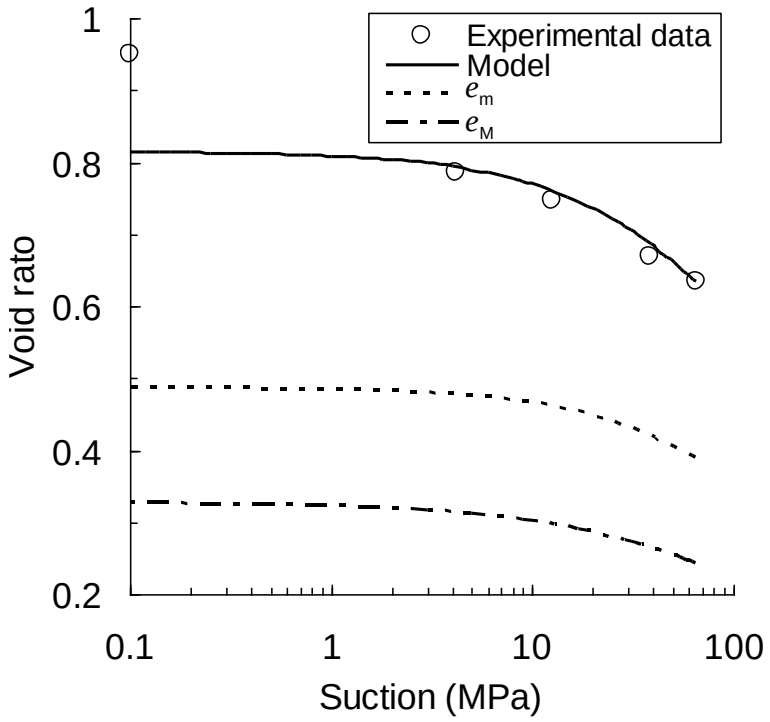

458

459 Figure 5. Void ratio changes upon wetting under a vertical stress of 0.1 MPa

460

461

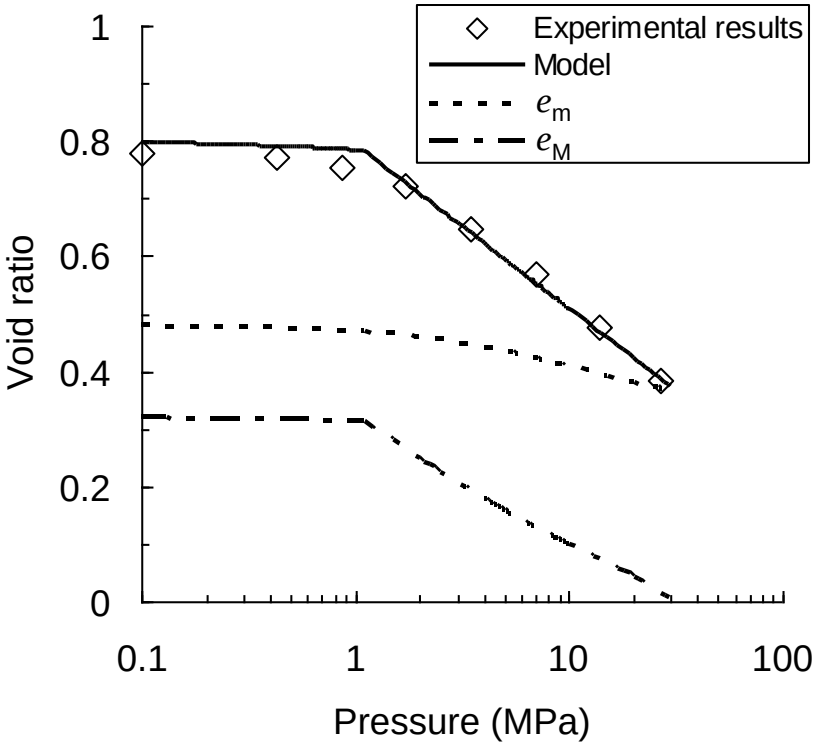

462

463 (a) s = 4.2 MPa

464

465

466

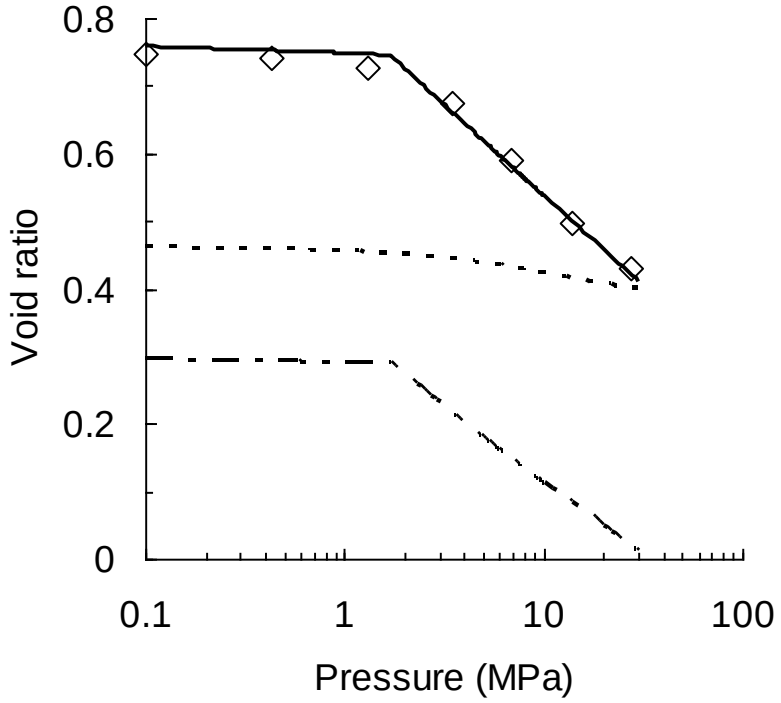

(b) s = 12.6 MPa

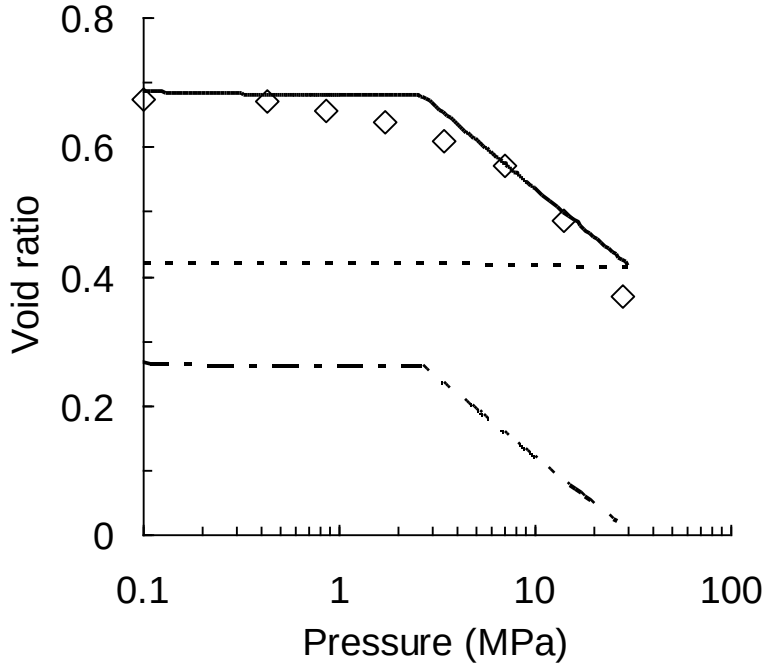

(c) s = 38 MPa

Figure 6. Void ratio changes upon mechanical loading at constant suction

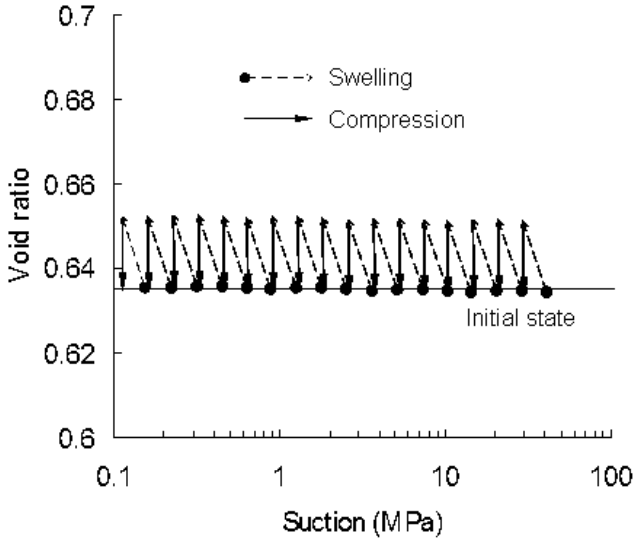

474

475 Figure 7. Stress path followed during the swelling pressure simulation

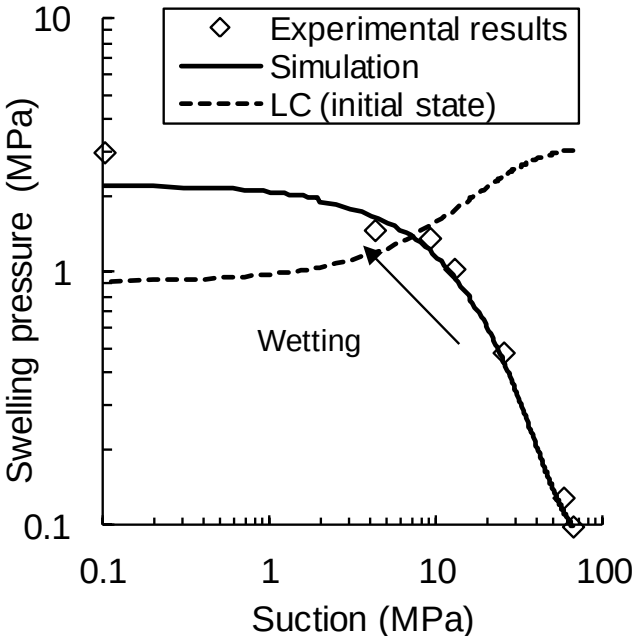

476

477 Figure 8. Changes of swelling pressure during suction decrease under constant volume
478 condition

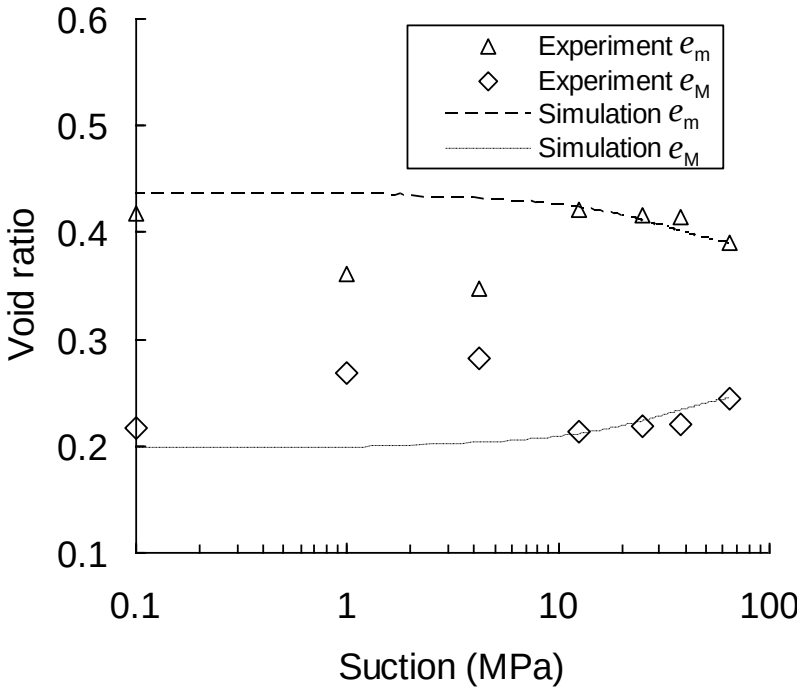

479

480 Figure 9. Changes in the e_m and e_M during suction decrease under constant volume condition

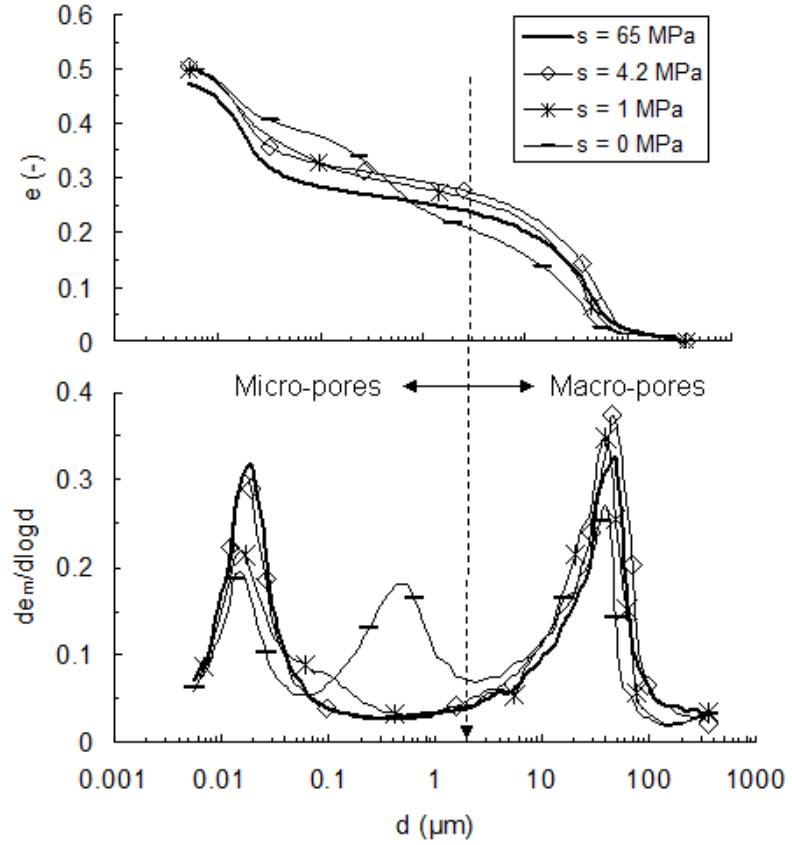

481

482 Figure 10 Pore size distribution changes

483

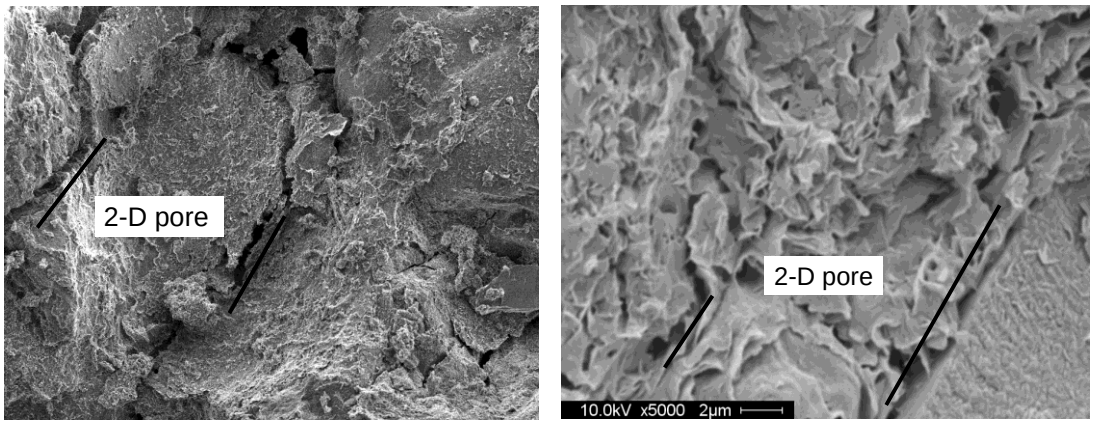

(a) (b)

Figure 11 2-D pores with diameter of 50μm (a) and 1μm (b)

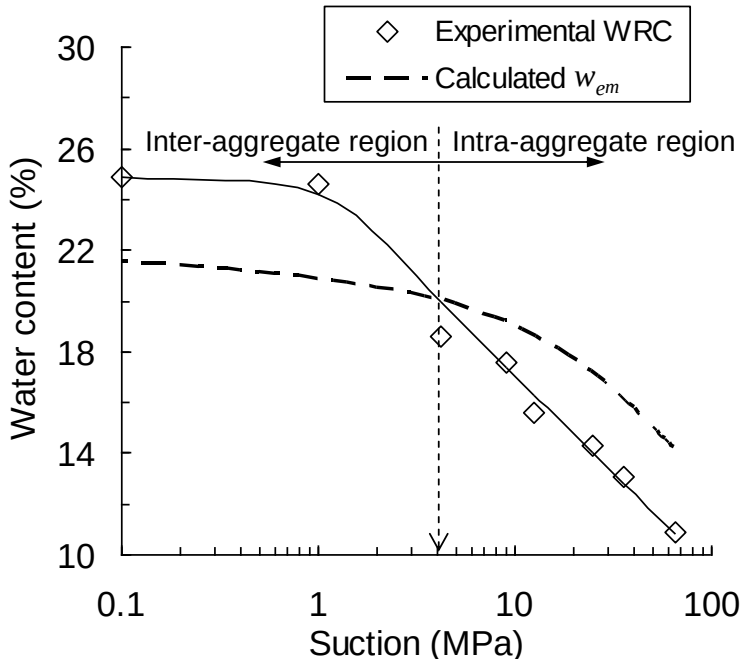

Figure 12. WRC and calculated micro-structural water content